

Ni induced few-layer graphene growth at low temperature by pulsed laser deposition

K. Wang,^{1,a} G. Tai,^{1,2} K. H. Wong,¹ S. P. Lau,¹ and W. Guo²

¹Department of Applied Physics and Materials Research Centre, The Hong Kong Polytechnic University, Hung Hom, Kowloon, Hong Kong SAR, China

²Institute of Nanoscience, Nanjing University of Aeronautics and Astronautics, 29 Yudao Street, Nanjing 210016, China

(Received 13 April 2011; accepted 28 May 2011; published online 13 June 2011)

We have used pulsed laser deposition to fabricate graphene on catalytic nickel thin film at reduced temperature of 650 °C. Non-destructive micro-Raman spectroscopic study on our samples, measuring 1x1 cm² each, has revealed few-layer graphene formation. Bi-, tri-, and few-layer graphene growth has been verified by High Resolution Transmission Electron Microscopy. Our experimental results imply that the number of graphene layers formation relies on film thickness ratios of C to Ni, which can be well controlled by varying the laser ablation time. This simple and low temperature synthesizing method is excellent for graphene based nanotechnology research and device fabrication. © 2011 Author(s). This article is distributed under a Creative Commons Attribution Non-Commercial Share Alike 3.0 Unported License. [doi:10.1063/1.3602855]

I. INTRODUCTION

Graphene is an ensemble of quasi-two-dimensional (2D) sp²-bonded carbon atoms in planar configuration.^{1–3} Numerous reports have indicated that it exhibits many unique and excellent electronic properties, for instance, the high charge carrier mobility and room temperature quantum Hall effect.^{4–7} Utilization of all these attractive and inspiring properties of graphene for practical purposes, however, relies on the availability of good and controllable fabrication technique. Historically, graphene was produced by micromechanical cleavage.⁵ At present, graphene syntheses mainly use thermal decomposition of a C containing material, such as SiC and C₆₀, and metal induced graphitization.^{8,9} Recent research focus is on developing preparation technique to produce graphene with controllable few-layer thickness. Graphitization of amorphous C (a-C) by using catalytic transition metals, such as cobalt (Co),¹⁰ platinum (Pt),^{10,11} ruthenium (Ru),¹² iridium (Ir)¹³ and nickel (Ni),^{14,15} is the most popular way to produce graphene. It has been known for many years that various forms of carbon were observed on metal surfaces after thermal treatment at elevated temperatures.^{16,17} The dominant mechanism involves the dissolution and precipitation of a-C in metal, which is similar to metal-mediated crystallization of silicon and germanium.^{18,19} The number of graphene layers thus formed relies on how much C precipitates from C-metal solid solution. As a result, a fine control of the thickness ratio of C to metal is crucial for the few-layer graphene formation. Up-to-date, chemical vapor deposition (CVD) is the most successful method to produce high quality graphene. It involves passing through hydrocarbon gases in a tube held at elevated temperature and a chemical reaction on the active metal surface. In most cases, the processing temperature needs to be as high as 1000 °C.^{8,9,20}

With the current fast growing interests in graphene-based nanotechnology, there are great demands on high quality few-layer graphene. We have developed a simple and fast processing technique based on pulsed laser deposition (PLD) to grow few-layer graphene at reduced temperature

^aAuthor to whom correspondence should be addressed. Electronic mail: wangkai369@hotmail.com



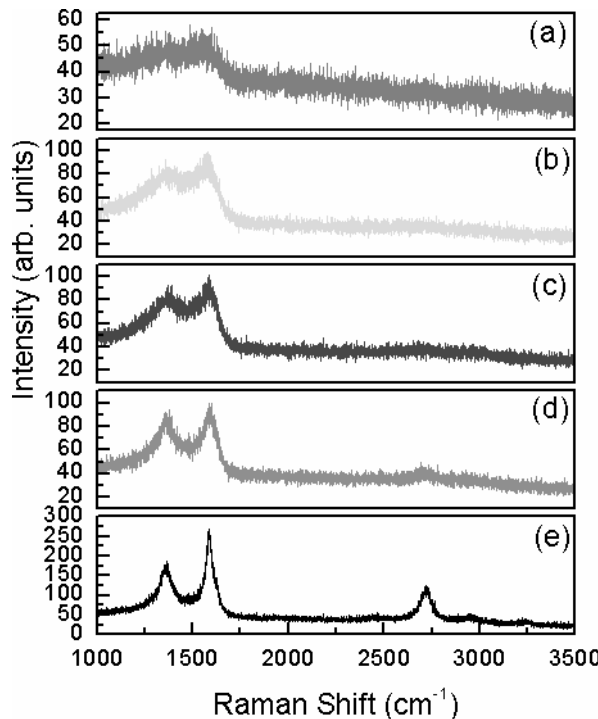


FIG. 1. Raman spectra of PLD-grown carbon on 120nm Ni thin films at (a) 300 °C. (b) 400 °C. (c) 500 °C. (d) 600 °C and (e) 650 °C.

of 650 °C on Ni thin film. These days, Ni, together with copper (Cu), have received the most attention as substrate materials for graphene growth. We chose Ni because it is inexpensive and is a standard material for electronic applications. In contrast to conventional PLD growth of C films, in which the concerns are mainly on the deposited C layer thickness, our work focuses on the fine control of the relative thicknesses of the deposited C and Ni films, and adatom diffusion. PLD is known to produce energetic atomic species with energy up to a few keV.²¹ It is therefore expected to promote C adatom diffusion into Ni at reduced substrate temperature. Furthermore, the C to Ni film thickness ratio can be controlled easily in PLD by altering the laser ablation time under fixed repetition rate or by using different laser irradiation fluences for C and Ni respectively. In these respects, controllable few-layer graphene growth can be obtained by PLD method at relatively low temperature.

II. EXPERIMENTAL

In the experiment, monocrystalline Si wafers coated with 300 nm SiO₂ were used as substrates. They were cut into 1x1 cm² pieces and cleaned with acetone, ethanol and de-ionized water. PLD was carried out in a stainless steel chamber evacuated to a base pressure of 2×10^{-6} Torr. A KrF laser ($\lambda = 248$ nm) operated at 4 Hz repetition rate was used throughout. For both Ni and C targets, the separation between the targets and the substrate was set to be 35 mm. The Ni thin films were deposited onto SiO₂ with pulsed laser fluence of 5.43 J/cm² (220 mJ) at room temperature. Immediately after the Ni deposition, the substrate temperature was raised to 650 °C without breaking the vacuum for 1 hour in order to enlarge the average grain size of Ni film. Afterward, a rotating graphite target was then ablated by the same laser with lower laser fluence of 4.40 J/cm² (180 mJ). The as-prepared sample was cooled down naturally to room temperature under vacuum without considering quick quenching of the substrate. All samples were studied by micro-Raman spectroscopy using a 488 nm laser as the excitation source. Graphene samples with and without lifting from the Ni films were examined by High Resolution Transmission Electron Microscopy (HRTEM) for definitive evaluation of few-layer graphene formation. For cross section TEM determination, a graphene sample was cut

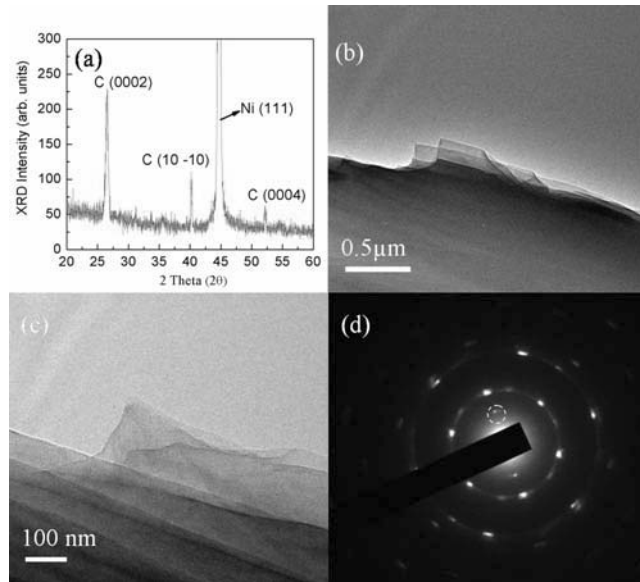


FIG. 2. (a) XRD spectrum for the sample structure Si/SiO₂/Ni (120 nm)/C (30 nm). (b) and (c) Low magnification TEM images for graphitic layer. (d) Selected area electron diffraction pattern.

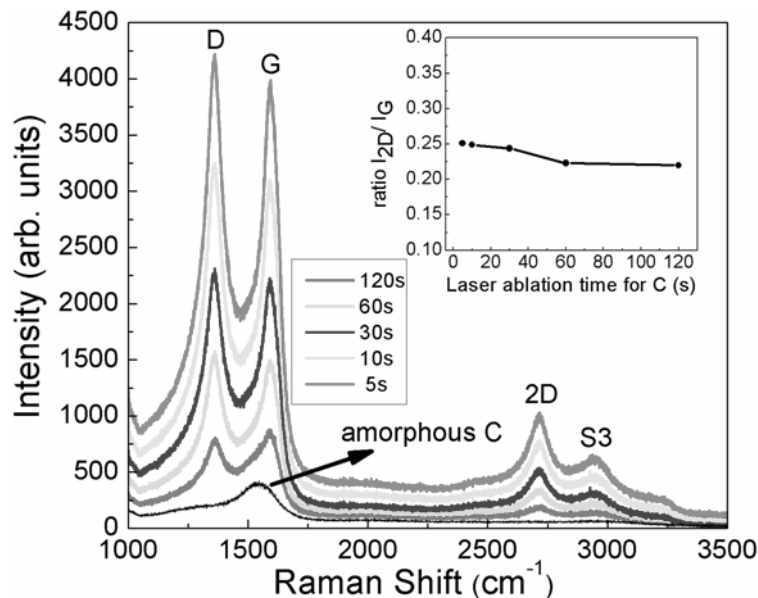


FIG. 3. (Color online) Raman spectra of PLD-grown graphene on 25nm Ni thin films for different laser ablation time of C. The inset shows the ratio of I_{2D}/I_G versus the laser ablation time of C.

into two small pieces. Both of them are stacked together firmly by protective epoxy. Afterward, the sample went through the normal polishing, dimpling and ion milling processes. The transfer of the PLD derived graphene on copper grid for TEM plane view was achieved by spin coating a very thin poly[methyl methacrylate] (PMMA) layer and wet-etching the Ni thin film with an aqueous HCl solution (5%) for 24 hours. After the sample has been closely attached to the TEM copper grid, the PMMA can be dissolved by exposing to acetone vapor for 4 to 5 hours. This transfer process allows graphene to maintain its continuity.²² In addition, Atomic Force Microscopy (AFM) was used to evaluate the height profile of graphene after it was transferred on SiO₂/Si substrate.

TABLE I. Raman intensities for I_D , I_G , I_{2D} , I_D/I_G and I_{2D}/I_G of Fig. 4.

Ni Ablation time (min)	Ni thickness (nm)	I_D (a.u.)	I_G (a.u.)	I_{2D} (a.u.)	I_D/I_G	I_{2D}/I_G
5	25	711.66	568.11	122.45	1.25	0.22
10	50	152.80	314.64	177.13	0.49	0.56
15	75	91.32	212.38	129.78	0.43	0.61

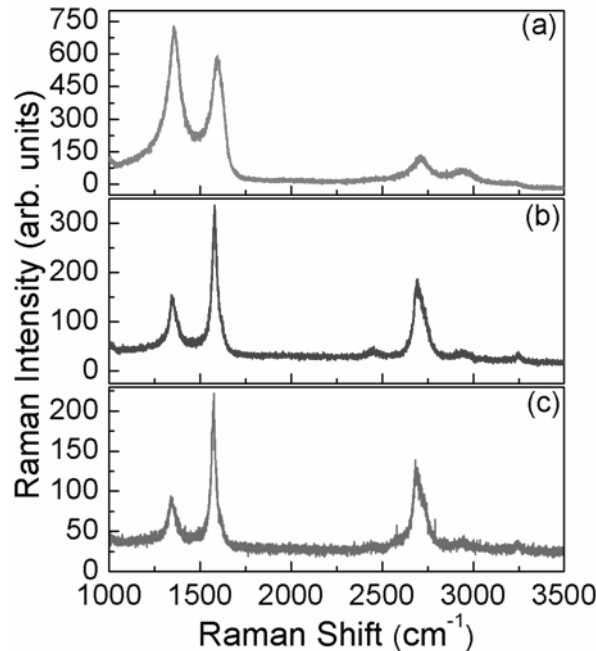


FIG. 4. Raman spectra of PLD-grown graphene on (a) 25 nm Ni film, (b) 50 nm Ni film and (c) 75 nm Ni film.

III. RESULTS AND DISCUSSION

It has been widely accepted that Raman spectroscopy is the most reliable, non-destructive and quick inspection for graphene.^{9,23} Figure 1 shows the Raman spectra of sample structure, Si/SiO₂/Ni (120 nm)/C (30 nm), at 5 different deposition temperatures of C. The thickness ratio of C to Ni was randomly chosen in order to investigate Ni induced graphitization temperature for PLD. From Figure 1(a) to 1(e), three remarkable peaks, around 1350 cm⁻¹, 1580 cm⁻¹ and 2700 cm⁻¹, are observed for samples fabricated at higher temperatures [Fig. 1(e)]. The Raman peak shown at about 1350 cm⁻¹ is due to defected graphite and it is usually called disorder-induced D band.²⁴ It originates from unorganized carbon domains and small graphite crystal size. The intensity of D band is associated with non-sp² bonding. Since Raman fundamental selection rule can not applied for zone-boundary phonons, the D band is not seen in the first order Raman spectra of defect-free graphite. The peak located at 1580 cm⁻¹ is graphitic G band. It represents the crystalline quality of graphite and evidences the formation a hexagonal lattice in graphite. For mono-crystalline graphite, only single line appears at 1580 cm⁻¹ and the G band is highly symmetric.²⁵ Thus, G denotes the symmetry-allowed graphite band. For the presence of amorphous C (a-C), the full width at half maximum (FWHM) of the G band is broad and the peak shifts to about 1540 cm⁻¹. The profile shown around 2700 cm⁻¹ is the graphite-like G band, which is a double resonance of D band. It is often denoted by 2D or G'. On the contrary, the 2D has nothing to do with the G peak; however, it represents the second order of zone-boundary phonons. In this figure, the sample with 300 °C has no obvious indication of crystalline phase for C. For the same sample structure fabricated at 400 °C, the Raman profile exhibits the appearance of D- and G-band. However, the G-band is broad and non-symmetric. Its intensity is comparative with the one of D-band. With increasing in the deposition temperature of C,

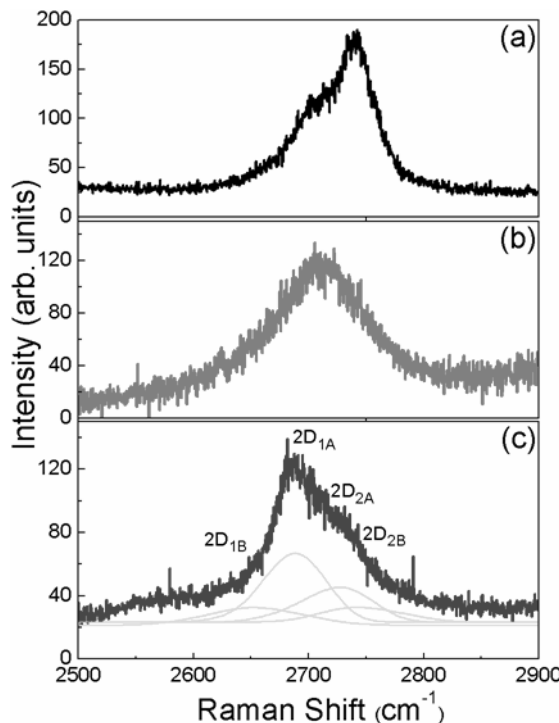


FIG. 5. 2D bands in Raman spectroscopy of (a) bulk graphite. (b) multi-layer graphene. (c) bi-layer graphene (four components of the 2D peak of bi-layer graphene).

we found the G-band tends to become narrow and symmetric. The result reflects higher temperature for carbon gives rise to relatively good crystallinity. In addition to this, the separation for both D- and G- bands tend to become distinguishable. In addition to this, we found a broad D-band for sample fabricated at 650 °C still exists, which gives a result of amount of defect. This reason is primarily due to non-sp² bond formation of C atoms. For the thickness ration of C to Ni which we have chosen here is not sufficient to demonstrate the reduction of D band. Therefore, we chose 650 °C as an appropriate temperature for C deposition in the following investigations.

Figure 2 shows the corresponding XRD and TEM images of the sample fabricated at 650 °C. In Figure 2(a), a sharp and intense Ni peak appears at 44.78°. Moreover, the Ni grains are all well aligned in the (111) direction after annealing at 650 °C. The XRD peak shown at 26.62° indicates hexagonal arrangement of graphitic (0002) lattice planes. Apart from this, the (10-10) and (0004) oriented lattice planes were also detected. Figure 2(b) and 2(c) show the top view of low magnification TEM images of graphitic layer. Smooth and homogeneous surfaces are clearly seen. The corresponding Selected Area Electron Diffraction (SAED) spot marked by the white dotted circle in Figure 2(d) proves the (0002) crystalline orientation of graphitic layers.

In order to investigate the effect of thickness ratio of C to Ni on graphene growth, C with different thicknesses (or different laser ablation time) were deposited onto 25 nm Ni thin films. The corresponding Raman spectra are shown in Figure 3. Despite those three bands which we have discussed previously, another band appears at 2900 cm⁻¹ and it is regarded as a combination of D and G peaks, or sometime called S3 peak.²⁶ Conventionally, the ratio, I_D/I_G, is used as a measure for the non-sp² to sp² bonding characteristics. Some previous reports have also suggested that the number of graphene layers is sensitive to the ratio I_{2D}/I_G.^{9,27} For this set of our samples with different amount of C depositions, their intensities of D band are almost the same as those of G band of crystalline phase C. Moreover, their ratios I_{2D}/I_G, which are plotted in the inset, are all around 1/4. This is a clear indication that multi-layer graphene (more than 5 layers) occurs in all samples. Judging from Figure 3, the sample with the least C deposition shows the strongest Raman signal. We believe that this is primarily due to the presence of non-dissolved a-C, which shields off some of the

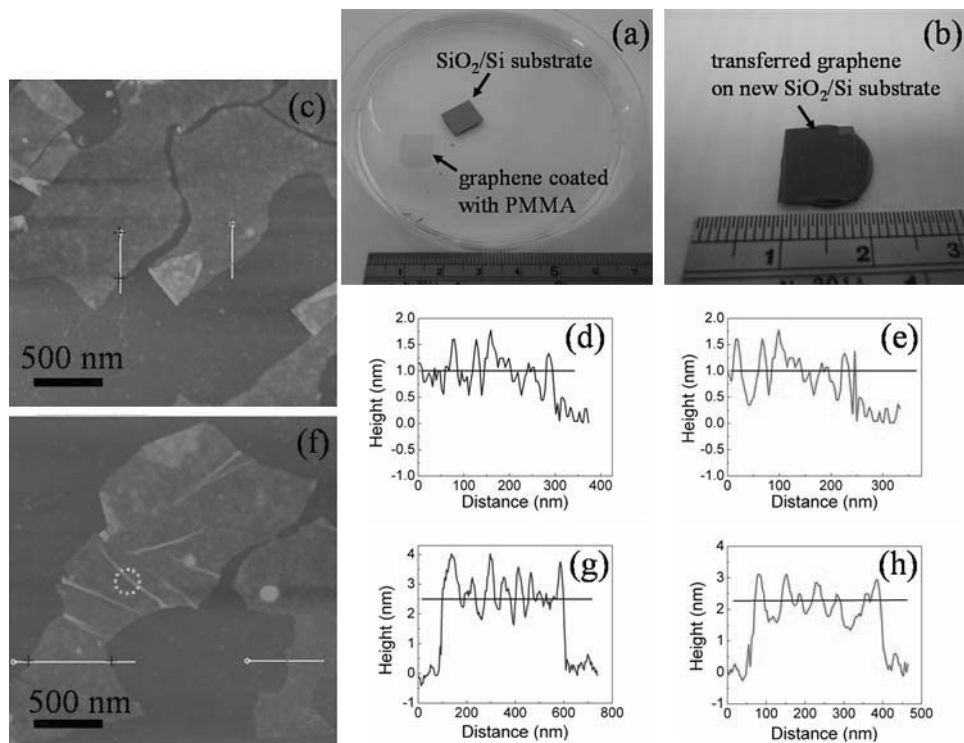


FIG. 6. (a) Photographic image for graphene transfer. (b) Graphene is transferred on a clean SiO_2/Si substrate. (c) AFM image for bi-layer graphene. (d) and (e) Height profiles taken along the blue and red solid lines for bi-layer graphene. (f) AFM image for tri-layer graphene. (g) and (h) Height profiles taken along the blue and red solid lines for tri-layer graphene.

excitation laser from irradiating onto the crystalline C at the interface. Indeed, the Raman band of a-C is conspicuously observable in the spectrum of the sample produced by 120 s of C deposition. Apparently, all of these samples have excessive C deposition. At 650 °C, their C saturation status in C-Ni solid solution is similar and high. When the samples are cooled to room temperature, substantial amount of C precipitate at the Ni film surface and form multi-layer graphene. In order to produce few-layer graphene (≤ 5 layers), we need to lower the initial C saturation status. Less C deposition and/or thicker Ni film are therefore desired. Further reduction of C deposition time (<5 s), however, one cannot guarantee a complete C coverage of the Ni film surface. An alternative is to use thicker Ni films.

Ni films were fabricated on SiO_2 by three different laser ablation time intervals of 5 mins, 10 mins and 15 mins corresponding roughly to 25 nm, 50 nm and 75 nm respectively. The deposition time for all the C layers was 1 min (~6 nm) in this experiment. The Raman spectra of these samples are shown in Figure 4. The intensities of I_D , I_G , I_{2D} and calculated ratios are given in Table I. In this case, the intensity ratio of I_D/I_G appears to decrease with increase in the Ni film thickness. We notice that for C deposited onto Ni thin films of 50 nm (10 mins) and 75 nm (15 mins), the I_{2D}/I_G intensity ratios are more than 50%, implying tri- and bi-layer graphene formations. Moreover, by contrary, the Raman profile of 75 nm Ni thin film gives significant decrease of D band intensity. It results in significant absence of defects at 650 °C. For a fixed amount of C deposited onto the Ni films at this given temperature, C saturation in C-Ni solid solution is easier to reach for the thinnest Ni film. It results in the smallest Ni volume. Thereby, in our case, the sample which was fabricated onto 25 nm Ni thin film will reach C supersaturation easily. When it is cooled to room temperature, the solubility of Ni tends to become weak. Consequently, less carbon is required to form solid solution with Ni films. The reduction of the solubility of Ni leads to C precipitation.¹⁷

Further evaluation of graphene layer was obtained by studies of the relative Raman shift of the 2D bands for bulk graphite, multi-layer graphene and bi-layer graphene. As seen from

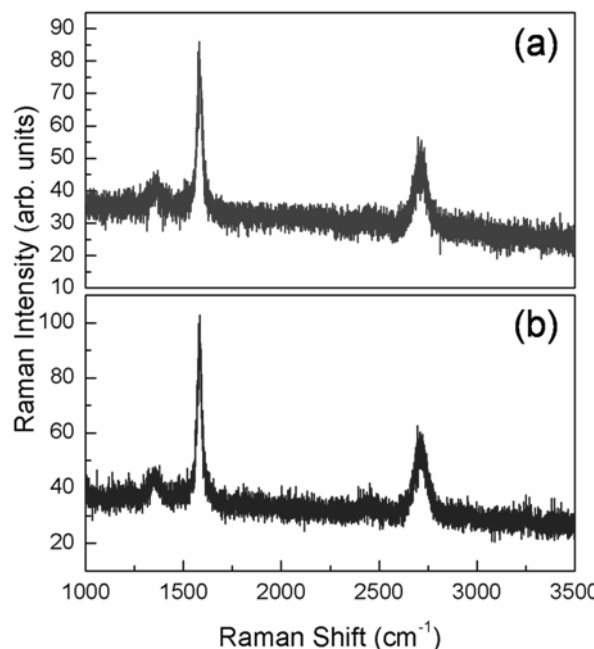


FIG. 7. (a) The corresponding Raman spectrum for bi-layer graphene on SiO_2/Si substrate (the same sample shown in Figure 6(c)). (b) The corresponding Raman spectrum for tri-layer graphene on SiO_2/Si substrate (the same sample shown in Figure 6(f)).

Figure 5(a)–5(c), the 2D band shifts from approximately 2739 cm^{-1} down to 2686 cm^{-1} . Both the Raman 2D profiles of bulk graphite and bi-layer graphene are asymmetric. Raman scattering is a fourth order process involving electron-phonon scattering. Due to the interaction of graphene planes, the 2D peak of bi-layer graphene splits into 4 components.^{28,29} As indicated in Figure 5(d), the 2D peak of our bi-layer graphene sample is, indeed, composed of four components, $2\text{D}_{1\text{B}}$, $2\text{D}_{1\text{A}}$, $2\text{D}_{2\text{A}}$ and $2\text{D}_{2\text{B}}$. Among these four, $2\text{D}_{1\text{A}}$ and $2\text{D}_{2\text{A}}$ have relatively higher intensities than the other two. The result can be directly compared with those of previous Raman spectroscopic study for bi-layer graphene.²³

After the catalytic Ni thin film was dissolved in FeCl_3 acid, the graphene layer coated PMMA was transferred out. Figure 6(a) shows the photographic image of graphene coated with PMMA detached from $\text{Ni}/\text{SiO}_2/\text{Si}$. The solution is diluted HCl, which can be used to further clean the residual Ni flakes on the graphene surface. Figure 6(b) displays the same graphene layer attached to a new SiO_2/Si substrate. The PMMA was removed by dipping the sample into acetone. From this image, few layer graphene coated on SiO_2 exhibits blue color. Two different samples followed the same transferring process were used for AFM examination. In Figure 6(c), two large pieces of graphene layers are shown in a $2\text{ }\mu\text{m}\times 2\text{ }\mu\text{m}$ area of AFM image. The break is due to scratch of large graphene for height profile measurement. Two different positions along each graphene layer were chosen. The corresponding height profiles are shown in Figure 6(d) and 6(e). Owing to the average thickness is around 1nm, both measurements indicate bi-layer graphene formation. Same method was applied for another sample and the AFM image is shown in Figure 6(f). The green dotted circle shows the present of graphene wrinkle. Its formation is due to the thermal expansion coefficient difference between Ni and graphene.⁸ From the height profiles of Figure 6(g) and 6(h), a slight increase in the thickness of graphene layer by approximately 1nm indicates 3 or 4 layers graphene formation. Furthermore, for both samples examined by AFM in Figure 6(c) and 6(f), the corresponding Raman spectra are displayed in Figure 7(a) and 7(b) respectively. Obviously, highly symmetric G bands indicate our transferred graphene samples have excellent crystallinity. The Raman intensity ratios of $I_{2\text{D}}/I_{\text{G}}$ for both Raman spectra in Figure 7(a) and 7(b) are 0.63 and

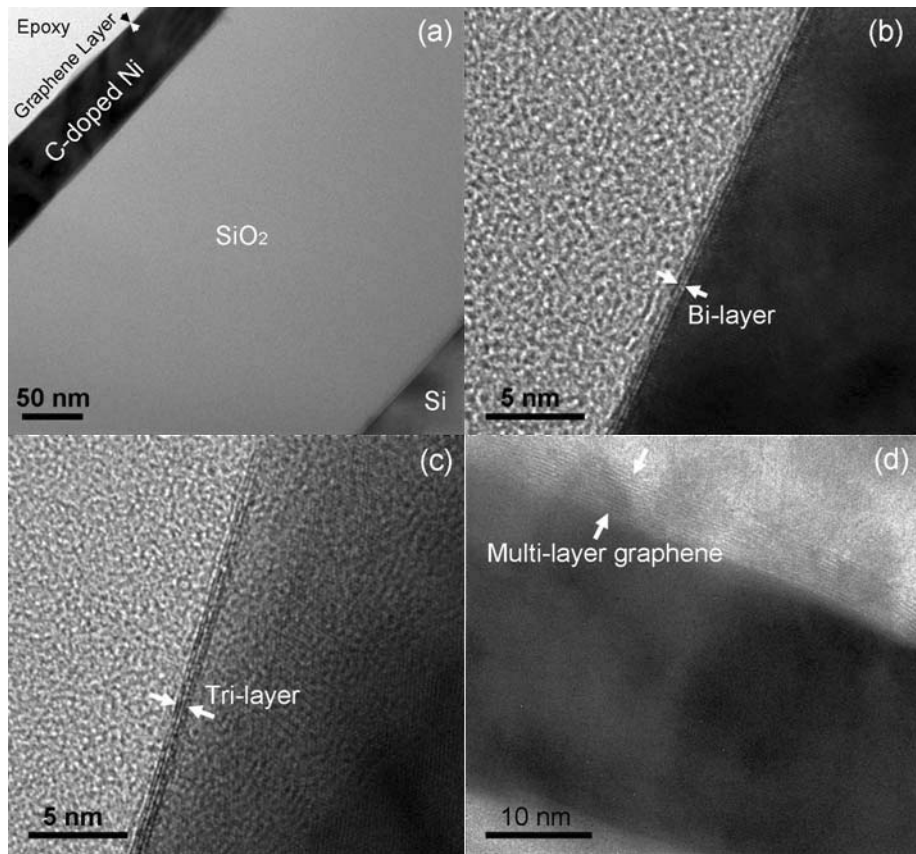


FIG. 8. TEM characterization of PLD-grown graphene films. (a) Low magnification TEM image showing PLD-grown graphene on Ni thin film. High resolution TEM images for (b) bi-layer graphene, (c) tri-layer graphene and (d) multi-layer graphene.

0.57, which confirm the presence of bi- and tri- layer graphene on the SiO_2/Si substrates. Further evaluation of the number of graphene layer was conducted using cross section HRTEM images in the following part.

Figure 8(a) displays the low magnification TEM image of the cross section of the graphene/Ni/ SiO_2/Si heterostructure. During laser ablation of the C target, the ejected C atoms were deposited on and adsorbed by the Ni layer. In lowering the substrate temperature, the amount of C segregates from Ni depends on the initial saturation status of C-Ni solid solution. The bi- and tri-layer graphene are clearly revealed in the HRTEM images of Figure 8(b) and 8(c). Clean and sharp interfaces with long range order between graphene layers and C-doped Ni thin films are indicated by those arrows. Both bi- and tri-layer graphene lie flat on the C-doped Ni top surface. Figure 8(d) displays the HRTEM image of multi-layer graphene grown on 25 nm Ni film. The HRTEM results thus strongly support our view that PLD is an excellent and simple technique for few-layer graphene growth.

IV. CONCLUSION

In summary, we have thus far demonstrated that few-layer graphene can be fabricated on Ni thin film at 650 °C by PLD. The crystalline graphene layer growth is based on Ni induced crystallization method. Both XRD and TEM reveal good crystallinity of graphitic layer and graphene. The number of graphene layers relies on thickness ratio of C to Ni, which can be controlled conveniently by tuning the laser ablation time. The non-destructive Raman spectroscopy has also revealed the distinct features of 2D band among bi-layer graphene, multi-layer graphene and bulk graphite. Therefore, our

few-layer graphene fabrication technique based on PLD is expected to be very useful for graphene research.

ACKNOWLEDGEMENT

This work was supported by a research grant of The Hong Kong Polytechnic University (PolyU J-BB9Q).

- ¹ A. K. Geim and K. S. Novoselov, *Nat. Mater.* **6**, 183 (2007).
- ² A. K. Geim, *Science* **324**, 1530 (2009).
- ³ P. Avouris, Z. Chen, and V. Perebeinos, *Nat. Nanotechnol.* **2**, 605 (2007).
- ⁴ I. A. Luk'yanchuk and Y. Kopelevich, *Phys. Rev. Lett.* **93**, 166402 (2004).
- ⁵ K. S. Novoselov, A. K. Geim, S. V. Morozov, D. Jiang, Y. Zhang, S. V. Dubonos, I. V. Grigorieva and A. A. Firsov, *Science* **306**, 666 (2004).
- ⁶ Y. Zhang, Y.-W. Tan, H. L. Stormer and P. Kim, *Nature* **438**, 201 (2005).
- ⁷ I. Meric, M. Y. Han, A. F. Young, B. Ozylimaz, P. Kim and K. L. Shepard, *Nat. Nanotechnol.* **3**, 654 (2008).
- ⁸ X. Li, W. Cai, J. An, S. Kim, J. Nah, D. Yang, R. Piner, A. Velamakanni, I. Jung, E. Tutuc, S. K. Banerjee, L. Colombo and R. S. Ruoff, *Science* **324**, 1312 (2009).
- ⁹ A. Reina, X. Jia, J. Ho, D. Nezich, H. Son, V. Bulovic, M. S. Dresselhaus and J. Kong, *Nano Lett.* **9**, 3087 (2009).
- ¹⁰ J. C. Hamilton and J. M. Blakely, *Surf. Sci.* **91**, 199 (1980).
- ¹¹ H. B. Lyon and G. A. Somorjai, *J. Chem. Phys.* **46**, 2539 (1967).
- ¹² J. T. Grant and T. W. Haas, *Surf. Sci.* **21**, 76 (1970).
- ¹³ B. E. Nieuwenhuys, D. I. Hagen, G. Rovida and G. A. Somorjai, *Surf. Sci.* **59**, 155 (1976).
- ¹⁴ M. Zheng, K. Takei, B. Hsia, H. Fang, X. Zhang, N. Ferralis, H. Ko, Y.-L. Chueh, Y. Zhang, R. Maboudian and A. Javey, *Appl. Phys. Lett.* **96**, 063110 (2010).
- ¹⁵ K. L. Saenger, J. C. Tsang, A. A. Bol, J. O. Chu, A. Grill and C. Lavoie, *Appl. Phys. Lett.* **96**, 153105 (2010).
- ¹⁶ Y. J. Yoon and H. K. Baik, *J. Alloys Compd.* **493**, 219 (2010).
- ¹⁷ J. Wintterlin and M. L. Bocquet, *Surf. Sci.* **603**, 1841 (2009).
- ¹⁸ O. Nast, T. Puzzer, L. M. Koschier, A. B. Sproul and S. R. Wenham, *Appl. Phys. Lett.* **73**, 3214 (1998).
- ¹⁹ Z. Tan, S. M. Heald, M. Rapposch, C. E. Bouldin and J. C. Woicik, *Phys. Rev. B* **46**, 9505 (1992).
- ²⁰ Z. Luo, Y. Lu, D. W. Singer, M. E. Berck, L. A. Somers, B. R. Goldsmith and A. T. Johnson, *Chem. Mater.* **23**, 1441 (2011).
- ²¹ A. D. Akhsakhalyan, Y. A. Bityurin, S. V. Gaponov, A. A. Gudkov and V. I. Luchin, *Sov. Phys. Tech. Phys.* **27**, 969 (1982).
- ²² L. Jiao, B. Fan, X. Xian, Z. Wu, J. Zhang and Z. Li, *J. Am. Chem. Soc.* **130**, 12612 (2008).
- ²³ A. C. Ferrari, J. C. Meyer, V. Scardaci, C. Casiraghi, M. Lazzeri, F. Mauri, S. Piscanec, D. Jiang, K. S. Novoselov, S. Roth and A. K. Geim, *Phys. Rev. Lett.* **97**, 187401 (2006).
- ²⁴ A. C. Ferrari and J. Robertson, *Phys. Rev. B* **64**, 075414 (2001).
- ²⁵ F. Tuinstra and J. L. Koenig, *J. Chem. Phys.* **53**, 1126 (1970).
- ²⁶ V. C. Tung, M. J. Allen, Y. Yang and R. B. Kaner, *Nat. Nanotechnol.* **4**, 25 (2009).
- ²⁷ Z. H. Ni, H. M. Wang, J. Kasim, H. M. Fan, T. Yu, Y. H. Wu, Y. P. Feng and Z. X. Shen, *Nano Lett.* **7**, 2758 (2007).
- ²⁸ A. C. Ferrari and J. Robertson, *Phys. Rev. B* **61**, 14095 (2000).
- ²⁹ S. Piscanec, M. Lazzeri, F. Mauri, A. C. Ferrari and J. Robertson, *Phys. Rev. Lett.* **93**, 185503 (2004).